Enhancement of Carrier Mobility in Semiconductor Nanostructures by Dielectric Engineering

Debdeep Jena[1] and Aniruddha Konar[2]

[1]Department of Electrical Engineering, University of Notre Dame, Notre Dame, Indiana 46556, USA
[2]Department of Physics, University of Notre Dame, Notre Dame, Indiana 46556, USA

(Received 28 September 2006; published 30 March 2007)

We propose a technique for achieving large improvements in carrier mobilities in 2- and 1-dimensional semiconductor nanostructures by modifying their dielectric environments. We show that by coating the nanostructures with high-κ dielectrics, scattering from Coulombic impurities can be strongly damped. Though screening is also weakened, the damping of Coulombic scattering is much larger, and the resulting improvement in mobilities of carriers can be as much as an order of magnitude for thin 2D semiconductor membranes, and more for semiconductor nanowires.

DOI: 10.1103/PhysRevLett.98.136805 PACS numbers: 73.63.−b, 73.50.−h, 77.22.−d

The dielectric mismatch between a nanoscale semiconductor material (relative dielectric constant ϵ_s) and the surrounding environment (ϵ_e) can result in a number of peculiarities not present in their bulk and layered forms (such as epitaxially grown quantum wells and superlattices). For example, recently it has been shown that in metallic carbon nanotubes there exist so-called "tubular image states" due to the strong attraction between external charges with their image states in the tube [1–3]. Furthermore, the dielectric-mismatch effect has been shown to be responsible for polarization-sensitive photocurrents in nanowires [4,5]. Keldysh had predicted from theoretical considerations that the Coulombic interaction potential between electrons and holes in nanoscale thin freestanding ($\epsilon_e = 1$) semiconductor films [6], and in freestanding nanowires [7], is strongly modified by the dielectric environment, resulting in a large enhancement in the excitonic binding energy. His prediction was recently experimentally confirmed [8,9]. Goldoni *et al.* proposed enhancement of excitonic binding energy in dielectric-semiconductor heterostructures by separate dielectric confinement of electric fields, and quantum confinement of carriers [10]. Because of the leakage of electric field lines originating from charges in the semiconductor nanostructure into the surrounding, a large degree of *tunability* of the optical properties of semiconductor nanostructures is possible by designing the dielectric environment.

The introduction of the concept of modulation doping by Dingle *et al.* in 1978 for epitaxially grown semiconductor heterostructures resulted in a major advance in achieving very high mobility 2-dimensional electron gases (2DEGs) [11]. Such 2DEGs have resulted in various fundamental discoveries in transport physics, and have also found many applications in high-speed transistor design. Over the past decade, major strides have been made in the bottom-up synthesis of various nanostructures, such as 0-dimensional (0D) nanocrystal quantum dots [12], 1D nanowires [13], and 2D nanoscale semiconductor sheets (for example, graphene [14–18], nanoribbons [19], etc.), which do not require the stringent lattice-matching requirements placed by epitaxy. In this work, we propose a novel technique for improving the electron mobility in such bottom-up 1D and 2D semiconductor nanostructures by showing that the dielectric environment has a profound effect on electron transport. Semiconductor nanowires [13] and nanosheets [15] are currently being investigated for possible usage in technologically important electronic devices such as transistors. Carrier mobility is an important parameter for such devices since it determines the power dissipation and switching speed. Proper design of the dielectric environment can result in drastic improvements in carrier mobilities in such structures. The availability of high-quality insulating materials with a very large range of relative dielectric constants ($1 < \epsilon_e < 300$) implies that the proposed technique of mobility improvement can be implemented with current technology.

We consider a thin 2D semiconductor membrane of nanoscale thickness in this work. To find the effect of the dielectric environment on electron mobility in the membrane, we first investigate its effect on Coulombic scattering of mobile charges from ionized impurity atoms located inside the membrane. A point charge e is located at $(0, 0, z_0)$ inside the semiconducting membrane of thickness a (see Fig. 1).

The dielectric mismatch and electric field penetration into the surrounding area results in a potential inside the membrane that can be found by a Green function solution of Poisson equation, or by the method of image charges. For the system here, an infinite series of point image charges form at points $z_n = na + (-1)^n z_0$, where $n = \pm1, \pm2, \ldots$. The nth point charge has a magnitude $e\gamma^{|n|}$, where $\gamma = (\epsilon_s - \epsilon_e)/(\epsilon_s + \epsilon_e)$ is a measure of the dielectric mismatch. The unscreened potential due to the Coulomb scatterer experienced by a mobile electron at a point $(\vec{\rho}, z)$ inside the membrane is then given by [20]

$$V_{\rm unsc}^{\rm Coul}(\rho, z) = \sum_{n=-\infty}^{\infty} \frac{e\gamma^{|n|}}{4\pi\epsilon_0\epsilon_s\sqrt{|\vec{\rho}|^2 + [z - z_n]^2}}. \quad (1)$$

The image charges are all of the same sign if $\epsilon_e < \epsilon_s$, and the effective potential seen by electrons in the membrane is *larger* than if there were no dielectric mismatch.

 © 2007 The American Physical Society

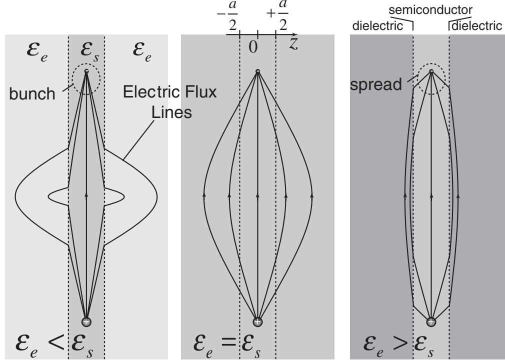

FIG. 1. Electric flux lines originating from a fixed ionized impurity and terminating on a mobile electron, and the effect of the dielectric environment. The flux lines bunch closer inside the semiconductor layer if $\epsilon_e < \epsilon_s$, and spread farther apart if $\epsilon_e < \epsilon_s$, thus enhancing Coulomb interaction in the former case and damping it in the latter.

The sign of image charges oscillate between positive and negative when $\epsilon_e > \epsilon_s$, and the total effective Coulomb potential seen is therefore smaller than if $\epsilon_e = \epsilon_s$ (shown schematically in Fig. 1).

Assuming that the surrounding dielectric provides a large energy barrier for confining electrons in the semiconductor membrane, the envelope function of mobile electrons occupying the n_z^{th} subband is given by $\Psi_{n_z,\mathbf{k}}(\vec{\rho}, z) = \phi_{n_z}(z)\chi_{\mathbf{k}}(\vec{\rho})$, where $\phi_{n_z}(z) = \sqrt{2/a}\cos(\pi n_z z/a)$, $\chi_{\mathbf{k}}(\vec{\rho}) = \exp(i\mathbf{k}\cdot\vec{\rho})/\sqrt{S}$, $\hbar\mathbf{k}$ being the in-plane quasimomentum, and S the area of the membrane. The matrix element for scattering from state $|n_z, \mathbf{k_i}\rangle \rightarrow |m_z, \mathbf{k_f}\rangle$ due to the unscreened Coulomb potential in Eq. (1) is given by an infinite sum of the Fourier transforms of the potentials due to the point charge and all its image charges $\tilde{V}_{\text{unsc}}^{\text{Coul}}(q) = \sum_{n=-\infty}^{\infty} \tilde{v}_n(q)$. Here $\tilde{v}_n(q)$ is the matrix term for the nth image charge, and is calculated to be

$$\tilde{v}_n(q, z) = \frac{e^2}{2\epsilon_0\epsilon_s q} e^{-q|z-z_n|}\gamma^{|n|}F_{n_z,m_z}(aq), \quad (2)$$

where $q = |\mathbf{k_i} - \mathbf{k_f}|$, and $F_{n_z,m_z}(aq)$ is a form factor arising from the quasi-2D nature of the electron gas. The form factor can be exactly evaluated for the envelope function used. $F_{n_z,m_z}(aq) \rightarrow 1$ both in the long-wavelength limit, as well as for very thin membranes ($a \rightarrow 0$). For thin membranes, the approximation $z_0 = 0$ is justified; under this approximation, the total contribution of all point charges can be exactly summed. We calculate the total unscreened potential seen by the mobile electron to be

$$\tilde{V}_{\text{unsc}}^{\text{Coul}}(q) = \frac{e^2}{2\epsilon_0\epsilon_s q}F_{n_z,m_z}(aq)\left[\frac{e^{qa} + \gamma}{e^{qa} - \gamma}\right]. \quad (3)$$

where the factor in rectangular brackets arises entirely due to the dielectric mismatch. In the long-wavelength limit, this factor approaches ϵ_s/ϵ_e, indicating that the *unscreened Coulomb interaction within the film is dominated by the dielectric constant of the environment* ($\tilde{V}_{\text{unsc}}^{\text{Coul}}(q) \sim e^2/2\epsilon_0\epsilon_e q$) *and not the semiconducting membrane.*

The other scattering mechanism that affects the mobility of carriers in very thin films is due to surface roughness (SR). Because of statistical fluctuations of atomic migration during the growth process, the thickness of such thin membranes can fluctuate randomly over monolayer thicknesses over the surface. Prange and Nee have shown that the roughness in the film thickness can be modeled by a function $\Delta a(\rho)$, which has a correlation $\langle\Delta a(\rho)\Delta a(\rho + \rho')\rangle_\rho = \Delta^2\exp(-|\rho - \rho'|^2/\Lambda^2)$, where Δ, Λ are the film thickness variation and the in-plane correlation length between the fluctuations, respectively, [21,22]. With such a model, the unscreened matrix element for SR intrasubband scattering for electrons within the m_z^{th} subband in the 2DEG is given by

$$\tilde{V}_{\text{unsc}}^{\text{SR}}(q) = \frac{\pi^{5/2}\hbar^2}{m^\star}\frac{\Delta\Lambda m_z^2}{a^3}e^{-(q\Lambda)^2/8}, \quad (4)$$

where $\hbar$ is the reduced Planck constant, and $m^\star$ is the electron effective mass.

The carrier mobility in the nanoscale membranes will be determined by the combined effect of Coulomb and SR scattering. For reasonably high impurity doping which is necessary for large intrinsic conductivity of the membrane, phonon scattering is weaker, and the reason for neglecting it is explained later. A careful look at the effect of the dielectric environment on the screening of the scattering potentials derived in Eqs. (3) and (4) is necessary for the evaluation of the total scattering rates. Screening by 2-dimensional electrons is captured in the $T \rightarrow 0$ limit by the Lindhard function [23]

$$\epsilon_{2d}(q, w) = 1 + \frac{e^2}{2\epsilon_0\epsilon_s q}\Pi(q, w)\Phi(q, a), \quad (5)$$

where Π is the polarization function and $\Phi(q, a)$ is a factor that depends on the subband index of screening carriers, ϵ_s, ϵ_e, membrane thickness a, and q. In the static Lindhard limit, the polarization function reduces to the 2D density of states $\Pi(q, \omega) \rightarrow m^\star/\pi\hbar^2$, and the dielectric-mismatch factor can be written as $\Phi = \Phi_1 + \Phi_2$ (see Ref. [24]). $\Phi_1(q, a)$ depends only on the scattering wave vector q and the semiconductor film thickness a, whereas $\Phi_2(q, a, \epsilon_s, \epsilon_e)$ also depends on the dielectric mismatch. We have evaluated the exact analytical expressions for Φ_1 and Φ_2 for the nanoscale membrane. The expressions are long, and will be presented in a more detailed paper; here, we mention some important features of the environment-modified dielectric screening function. For the rest of this work, we consider the electric quantum limit, i.e., for intrasubband scattering within the first subband ($n_z = m_z = 1$).

In the long-wavelength limit, $\Phi_1 \rightarrow 1$, and $\Phi_2 \rightarrow \epsilon_s/\epsilon_e - 1$. The screening function for a general (q, a) is written as $\epsilon_{2d}^{\text{eff}}(q) = 1 + q_{\text{TF}}^{\text{eff}}/q$ in analogy to the 2D screening function in the absence of dielectric mismatch

$[\epsilon_{2d}(q) = 1 + q^0_{\rm TF}/q]$. Here $q^0_{\rm TF}(q^{\rm eff}_{\rm TF})$ is Thomas-Fermi screening wave vector for the 2DEG without (with) dielectric mismatch. The ratio $q^{\rm eff}_{\rm TF}/q^0_{\rm TF}$ that captures the effect of the dielectric mismatch on screening is plotted in Figs. 2(a) and 2(b) for a GaAs thin film ($m^\star = 0.067m_0$, $\epsilon_s = 12.5$). Finite-temperature effect ($T = 300$ K) has been considered using Maldague's technique (see Ref. [22]). As can be seen, screening is enhanced if $\epsilon_e < \epsilon_s$, and reduced if $\epsilon_e > \epsilon_s$ due to the dielectric mismatch. Evidently, screening opposes the change in Coulomb interaction between charges due to the dielectric environment. Furthermore, the ratio approaches ϵ_s/ϵ_e at the limit of very small film thickness, implying that screening in a very thin 2D film is mediated entirely by the dielectric environment.

The dielectric-mediated screening changes each scattering potential to $\tilde{V}^i_{\rm scr}(q) = \tilde{V}^i_{\rm unsc}(q)/\epsilon^{\rm eff}_{2d}(q)$, and the momentum scattering rate for the ith scattering mechanism is given by

$$\frac{1}{\tau_i(E_k)} = \frac{2\pi}{\hbar}\int\frac{d^2k'}{(2\pi)^2}|\tilde{V}^i_{\rm scr}|^2(1-\cos\theta)\delta(E_k - E_{k'}), \quad (6)$$

where $\cos\theta = \mathbf{k_i}\cdot\mathbf{k_f}/|\mathbf{k_i}|\cdot|\mathbf{k_f}|$, $k = |\mathbf{k_i}|$, $k' = |\mathbf{k_f}|$, and the scattering rate is evaluated over the final density of states. A parabolic dispersion with effective mass $m^\star$ is used. Since both Coulombic and SR scattering are elastic, Matheissen's rule can be applied to evaluate the total scattering rate $(1/\langle\tau\rangle = 1/\tau_{\rm Coul} + 1/\tau_{\rm SR})$, and the Drude mobility is then given by $\mu = e\langle\tau\rangle/m^\star$.

We first investigate the effect of the dielectric environment on Coulomb scattering. The scattering rate for a 2DEG of density $n_{2d} = 10^{12}/{\rm cm}^2$ due to randomly distributed Coulombic point scatterers of the same density ($n_{\rm imp} = n_{2d}$) in a nanoscale GaAs membrane is shown

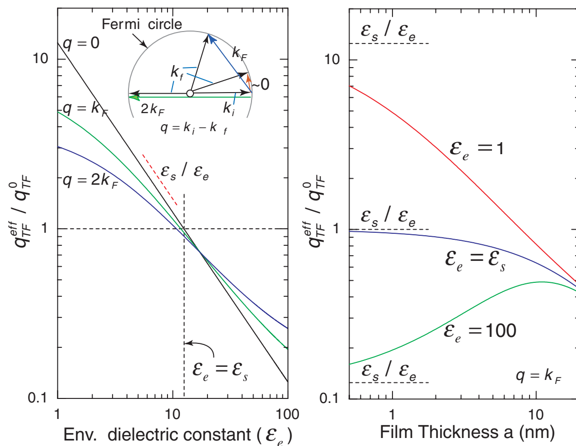

FIG. 2 (color online). The effect of dielectric mismatch on the Thomas-Fermi screening wave vector. (a) shows that screening is stronger than the case without dielectric mismatch for $\epsilon_e < \epsilon_s$ for small angle scattering ($q \sim 0$), $q = k_F$, and backscattering $q = 2k_F$ (for $a = 1$ nm). When $\epsilon_e < \epsilon_s$, screening is weaker than the case without dielectric mismatch. (b) shows that the effect of dielectric mismatch on screening is substantial if the thickness of membrane is small.

Fig. 3. The carrier density chosen ensures the electric quantum limit for the range of membrane thicknesses considered here. Figure 3(a) shows the effect on the scattering rate as the dielectric constant of the environment is changed. For very thin layers ($a = 1$ nm), the scattering rate exhibits a very strong dependence on ϵ_e, reducing $\sim$20 times from 66 ps^{-1} to 3 ps^{-1} as the environmental dielectric constant changes from $\epsilon_e = 1$ (semiconductor film in air) to $\epsilon_e = 100$ (film coated by a high-κ dielectric). As the film thickness increases, the effect of the dielectric mismatch on Coulombic scattering diminishes, and this feature is shown explicitly in Fig. 3(b). As the film thickness approaches $a = 20$ nm, Coulombic scattering becomes bulklike, and the dielectric mismatch has no effect beyond this thickness.

Hence, Coulombic scattering in membranes below a critical thickness [given in the long-wavelength limit by $a_{cr} \sim a^\star_B\epsilon_e/(\epsilon_e + \epsilon_s)$, $a^\star_B$ being the hydrogenic Bohr radius in the bulk semiconductor] can be strongly suppressed by coating the semiconductor layer with insulating dielectric barriers with high $\epsilon_e (> \epsilon_s)$. On the other hand, a free-standing ($\epsilon_e = 1$) doped semiconductor membrane will suffer from enhanced Coulombic scattering. For a GaAs nanoscale film, the strength of Coulombic scattering can be reduced by more than a factor of 20 for $a = 1$ nm. Similar results can be obtained for membranes made of other semiconducting materials.

In Fig. 4(a), we plot the total scattering rate by combining the effects of surface roughness and Coulombic scattering for three different dielectric environments. The surface roughness parameters used are 1 monolayer thickness variations $\Delta = 0.283$ nm, with an in-plane correlation length $\Lambda = 40$ nm (these values are typical for GaAs quantum wells (see Ref. [22]). The 2D electron gas density and the impurity density are both set to 10^{12} cm^{-2}. Under such conditions, impurity and SR scattering is found to be

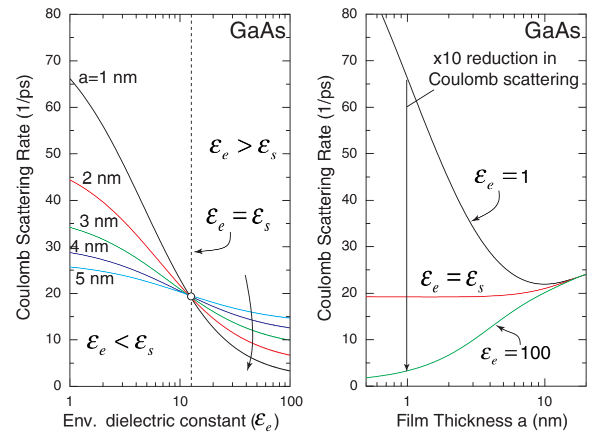

FIG. 3 (color online). (a) The variation of Coulombic scattering rate for different semiconductor layer thicknesses for a range of dielectric environments. (b) Effect of dielectric mismatch on Coulombic scattering as a function of the semiconductor membrane thickness.

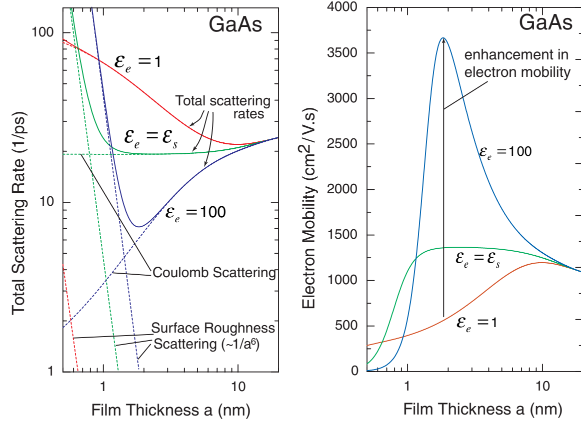

FIG. 4 (color online). (a) Total scattering rate due to combined surface roughness and Coulombic impurity scattering, and (b) the dependence of the total mobility for three dielectric environments on the semiconductor membrane thickness. A large increase in mobility is expected for thin semiconductor layers coated by high-κ dielectrics.

much stronger than polar optical phonon scattering (LO phonon scattering rate for GaAs is $\sim 2\ \mathrm{ps}^{-1}$ at room temperature), justifying its exclusion in the analysis. Since SR scattering has a a^{-6} dependence on the membrane thickness, it dominates for a <1 nm for GaAs. The strong dependence of SR scattering on the dielectric environment is entirely due to the dielectric-mismatch effect on screening, since the unscreened SR scattering matrix element [Eq. (4)] is not affected by the dielectric mismatch.

When the two processes are combined, the total scattering rate is lower compared to the bulk limit if $\epsilon_e > \epsilon_s$, and the thickness of the membrane is $a_{\min} < a < a_{cr}$, where $a_{\min}$ is set by the surface roughness. For atomically flat surfaces (for example, graphene), $a_{\min} = 0$ nm. The corresponding electron mobilities for the GaAs membrane are plotted in Fig. 4(b). For $a > 1$ nm, the mobility can be improved by coating the film by high-κ dielectrics; an enhancement as large as by a factor of 7 is possible by choosing ($\epsilon_e = 100$) for the GaAs membrane considered. The mobility is enhanced in general for ($\epsilon_e > \epsilon_s$) due to dielectric-mediated lowering of Coulomb scattering within the thickness window, the lower limit of which is set by the surface roughness, and the upper limit by the effective Bohr radius. Thus, large enhancements in carrier mobility are achievable in this fashion for membranes made from a wide range of semiconductors.

Relaxing the infinite barrier approximation leads to an increase of the electron effective mass, which can reduce the mobility. This correction is numerically evaluated for typical barrier heights (≥ 1 eV), and found to be small enough to be neglected. The dielectric constant of a material which has only an electronic contribution to the polarization scales inversely with the (direct) band gap [25]. To provide the confining potential for electrons assumed in this work, one can choose high-κ dielectrics in which the ionic contribution is substantially larger. Choice of such dielectrics (primarily oxides) implies that the polaronic dressing of the electron effective mass might offset the enhancement in mobility predicted. Such an increase is evaluated to be less than 10% for a wide range of ionic dielectrics, implying that the dielectric-mismatch induced giant enhancement in mobility persists. Deposition of high-κ dielectrics on nanoscale membranes can induce changes in the electron effective mass due to strain—this effect can be addressed by using the correct effective mass in the theory.

In conclusion, doped nanostructures suffer from enhanced Coulombic impurity scattering if they are freestanding. The electron mobility in such structures can be improved drastically by coating them with high-κ dielectrics. The large sensitivity of carrier mobilities in such membranes to the dielectric environment can be exploited for sensor applications. Finally, we note that the effect of dielectric mismatch on carrier scattering and mobility in ultrathin semiconductor nanowires is expected to be even stronger than in the nanoscale membranes considered here due to much stronger field penetration into the environment and weaker screening in 1D transport than in 2D. Therefore, the improvement of carrier mobilities for semiconductor nanowires by dielectric engineering will be higher than what is found here for 2D membranes. This is an attractive route for improving the performance of nanostructured electronic devices.

Support from NSF CAREER and from the ONR (Dr. Chagaan Bataar) for this work is acknowledged.

[1] B. E. Granger *et al.*, Phys. Rev. Lett. **89**, 135506 (2002).
[2] M. Zamkov *et al.*, Phys. Rev. Lett. **93**, 156803 (2004).
[3] D. Segal *et al.*, Phys. Rev. Lett. **94**, 016402 (2005).
[4] J. Wang *et al.*, Science **293**, 1455 (2001).
[5] A. Shabaev *et al.*, Nano Lett. **4**, 1821 (2004).
[6] L. V. Keldysh, JETP Lett. **29**, 658 (1979).
[7] L. V. Keldysh, Phys. Status Solidi A **164**, 3 (1997).
[8] E. A. Muljarov *et al.*, Phys. Rev. B **62**, 7420 (2000).
[9] V. S. Dnesprovskii *et al.*, JETP **87**, 382 (1998).
[10] G. Goldoni *et al.*, Phys. Rev. Lett. **80**, 4995 (1998).
[11] R. Dingle *et al.*, Appl. Phys. Lett. **33**, 665 (1978).
[12] D. V. Talapin *et al.*, Science **310**, 86 (2005).
[13] J. Xiang *et al.*, Nature (London) **441**, 489 (2006).
[14] T. Ohta *et al.*, Science **313**, 951 (2006).
[15] B. Obradovic *et al.*, Appl. Phys. Lett. **88**, 142102 (2006).
[16] C. Berger *et al.*, Science **312**, 1191 (2006).
[17] K. S. Novoselov *et al.*, Nature (London) **438**, 197 (2005).
[18] Y. Zhang *et al.*, Phys. Rev. Lett. **94**, 176803 (2005).
[19] D. Y. Khang *et al.*, Science **311**, 208 (2006).
[20] M. Kumagai *et al.*, Phys. Rev. B **40**, 12 359 (1989).
[21] R. E. Prange *et al.*, Phys. Rev. **168**, 779 (1968).
[22] H. Sakaki *et al.*, Appl. Phys. Lett. **51**, 1934 (1987).
[23] F. Stern, Phys. Rev. Lett. **18**, 546 (1967).
[24] B. A. Glavin *et al.*, Phys. Rev. B **65**, 205315 (2002).
[25] J. M. Ziman, *Principles of the Theory of Solids* (Cambridge University, Cambridge, England, 1972), 2nd ed.